Electronic Supplementary Material (ESI) for RSC Advances.

Effect of annealing atmosphere on quaternary chalcogenides based counter electrodes in dye-sensitized solar cells performance: Synthesis of Cu_2FeSnS_4, Cu_2CdSnS_4 nanoparticles by thermal decomposition process

Krishnaiah Mokurala * and Sudhanshu Mallick

Department of Metallurgical Engineering & Materials Science, Indian Institute of Technology Bombay, Mumbai-400076

Email address:krishna887@iitb.ac.in, Telephone number: +912225767641, Fax: +912225726975

Supporting information

2.1 Materials

$Cu(CH_3COO)_2.H_2O$ (SRL, AR Grade), $(Fe(NO_3)_3\ 9H_2O$ (Thomas Baker, AR grade), $Cd(CH_3COO)_2.2H_2O$ (SD fine, AR Grade) , $SnCl_2.2H_2O$ (Merck, GR grade), $CS(NH)_2$ (SD fine, AR grade), and CH_3CH_2OH (Merck, AR grade) were raw materials used for synthesis of quaternary chalcogenides nanomaterials via thermal decomposition process.

Electrolyte composition used in Dye-sensitized solar cells

The electrolyte is composed of the following chemicals: 0.1M lithium iodide (LiI, Anhydrous, Merck), 0.05M Iodine ((I_2, Thomas Baker, LR), 0.5M 4-tert-Butylpyridine (TBP, Sigma-Aldrich, 96%) and 0.6 M 1-Methyl- 3-propylimidazolim iodide (PMII, Sigma-Aldrich, 98%) and acetonitrile. Fluorine-doped tin oxide (FTO) substrates (TEC 8, sheet resistance 8 Pilkington).

Fabrication of photoanode and DSSCs assembly

The homogeneous TiO_2 slurry was obtained by pot milling of 3.6 g TiO_2 powder (P 25, Degussa), 3.6 ml of polyethylene glycol (i.e. PEG 600) (Merck) together with ethanol for 30 days. The prepared TiO_2 slurry was coated over the as-deposited compact layer of TiO_2/FTO substrate (5mmx5mm) by doctor blade technique. The films were dried at 125-130^oC for 1 h and then sintered at 500^oC for 30 min. This coating process was repeated multiple times to obtain the desired thickness (16μm). The sintered TiO_2 films were immersed in 0.3mM N719 dye (Dyesol) in ethanol for 24 h at room temperature for sufficient dye adsorption. The films were then rinsed with ethanol to remove the excess dye adsorbed. The films were then rinsed with ethanol to remove the excess dye adsorbed. DSSCs were assembled using the dye loaded TiO_2 film as photoanode and CCdTS /CFTS film based CE respectively. A spacing of approximately 60 μm was maintained between the electrodes using a Surlyn spacer, sandwiched between the electrodes. This gap between the electrodes was finally filled with the electrolyte.

Table S1 Crystalline size of the CFTS and CCdTS nanoparticles synthesized at different temperature for 1h

Synthesis temperature/1h	**CFTS nanoparticles (crystalline sizes (nm))**	**CCdTS nanoparticles (crystalline sizes (nm))**
300°C	8 nm	6 nm
350°C	13 nm	9 nm
400°C	17 nm	15 nm
450°C	21 nm	19 nm
500°C	26 nm	23 nm

Table S2: EDS analysis of CCdTS nanoparticle synthesized at different temperatures for 1 h

Synthesis temperature	**300°C**	**350°C**	**400°C**	**450°C**	**500°C**
Cu (atomic %)	25.5	26.0	26.4	26.7	26.9
Cd (atomic %)	13.7	13.2	13.0	12.5	12.0
Sn (atomic %)	14.5	13.5	12.7	12.2	11.0
S (atomic %)	46.3	47.3	47.9	48.6	50.1

Table S3: EDS analysis of CFTS nanoparticles synthesized at different temperatures for 1 h

Synthesis temperature	**300°C**	**350°C**	**400°C**	**450°C**	**500°C**
Cu (atomic %)	25.5	26.0	26.3	26.5	26.8
Fe (atomic %)	15.5	13.5	13.2	13.0	12.5
Sn (atomic %)	14.0	13.2	12.5	12.0	11.4
S (atomic %)	45.0	47.3	48.0	48.5	49.3

Table S4: EDS analysis of CCdTS films annealed at 525°C for 30 min in different atmosphere

Different atmosphere	**Film annealed in N_2 atm**	**Sulfurized films**
Cu (atomic %)	28.5	24.2
Cd (atomic %)	14.7	12.5
Sn (atomic %)	10.7	12.7
S (atomic %)	46.0	50.6
Cu/(Cd+Sn)	1.12	0.96
Cd/Sn	1.37	0.98
S/(Cu+Cd+Sn)	0.85	1.02

Table S5: EDS analysis of CFTS films annealed at 525°C for 30 min in different atmosphere

Different atmosphere	**Film annealed in N_2 atm**	**Sulfurized films**
Cu (atomic %)	28.0	23.4
Fe (atomic %)	15.2	13.0
Sn (atomic %)	10.4	12.5
S (atomic %)	46.4	51.4
Cu/(Fe+Sn)	1.09	0.91
Fe/Sn	1.46	1.04
S/(Cu+Fe+Sn)	0.86	1.05

1 Stability assessment of Counter electrodes

According to the reported literature, successive CV scanning, EIS scanning, long-term stability, under dark and illumination current-voltage test and removal rate of the films (mechanical stability) are used to examine the preliminary stability of various CEs. Mechanical stability (adhesion of CEs to substrates (FTO)), chemical stability (inert)/dissolution study and successive CV scanning of CEs are reported for stability assessment of CEs in the present study.

1 Mechanical stability of CEs

Lifetime of DSSCs depends on adhesion between CE/FTO interface. The adhesion test was performed by using ultrasonicator. The S–CCdTS-CE and S–CFTS-CE were immersed in ethanol and subjected to ultrasonication for 1 h. These CEs are periodically observed after 15 min. As observed from Fig. S1and Fig. S2, no major changes are noticed in both the CEs after 1 h. This indicates that the CEs are mechanical stability (well adherent to the FTO substrate).

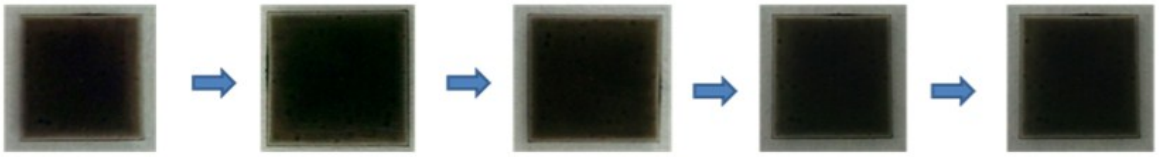

Fig. S1 Photographs of S–CFTS-CE each after 15 min of ultrasonication, respectively

Fig. S2 Photographs of S–CCdTS-CE, each after 15 min of ultrasonication, respectively

2 Chemical inertness (stability)/Dissolution study:

S–CFTS CEs and S–CCdTS-CEs were immersed in iodine base electrolyte for 14 days to study the dissolution of prepared CEs (Fig. S3). These CEs are periodically observed after 7

days. These CEs does not dissolve in electrolyte even after 14 days which indicates that these CEs are stable (inert) in iodine-based electrolyte (Fig. S4 and Fig. S5).

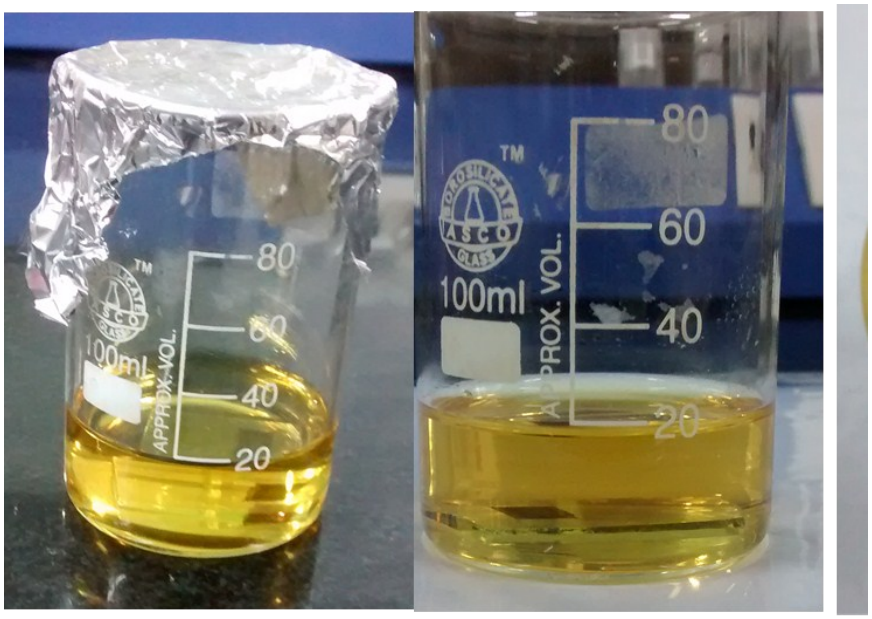

Fig. S3 Photographs of immersed S–CFTS CEs and S–CCdTS-CEs in an iodine based electrolyte and kept for 14 days study dissolution of prepared CEs

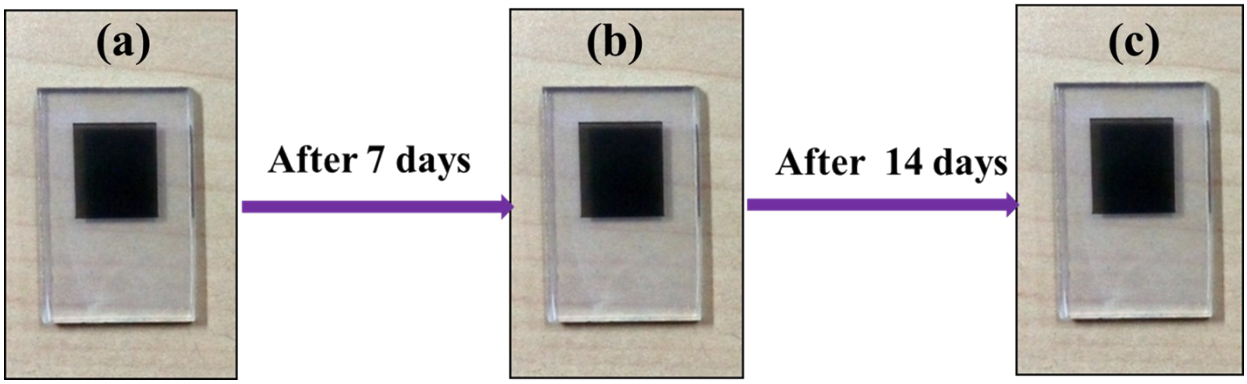

Fig. S4 Photographs of immersed S–CFTS CEs in iodine-based electrolyte: (a) Fresh, (b) after 7 days and (c) after 14 days

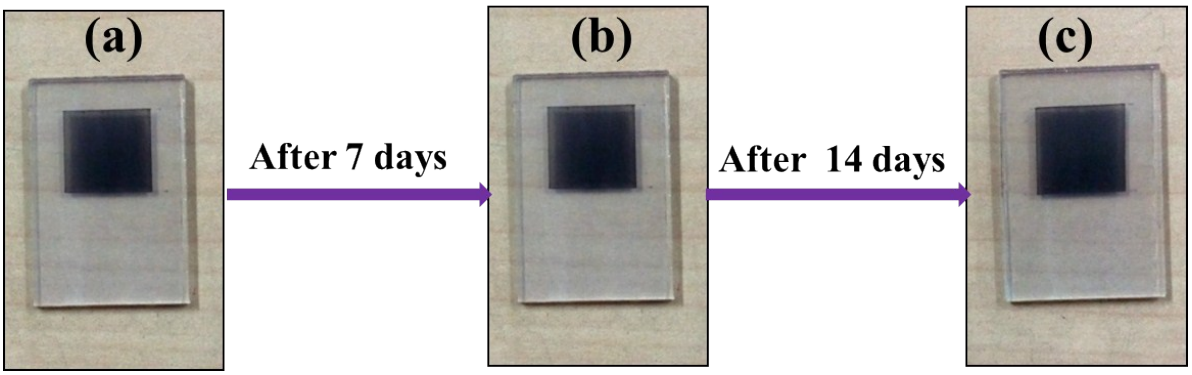

Fig. S5 Photographs of immersed S–CCdTS-CEs in iodine-based electrolyte : (a) Fresh S–CCdTS-CEs CE, (b) after 7 days and (c) after 14 days

2 Electrochemical impedance spectroscopy (EIS) and Tafel polarization measurements of counter electrodes

Electrocatalytic activity of CEs is further confirmed by EIS and Tafel polarization measurements. EIS and Tafel polarization measurements of symmetric cells of CEs are performed under illumination at zero bias voltage. The recorded EIS spectra are shown in Fig. S6 and the equivalent circuit (inset Fig. S6) is fitted with the help of zsimp software. Electrochemical parameters such as series resistance (R_s), charge-transfer resistance (R_{ct}) and the corresponding constant phase angle (CPE) at electrolyte/ CEs interface estimated from the EIS spectra are given in Table S6. The high-frequency intercept on the real axis represents the ohmic series resistance (R_s) of CEs. The radius of semicircle in the high-frequency region corresponds to the charge transfer resistance (R_{ct}) and the corresponding constant phase angle (CPE) at electrolyte/ CEs interface for I_3^- to I^- reaction. The semicircle at low-frequency range attributes to Warburg diffusion impedance (W) of the triiodide/iodide couple in the electrolyte. R_{ct} value of S S–CFTS CEs (2.9 Ωcm^2) and S–CCdTS-CEs (3.8 Ωcm^2) are found to be smaller than that N–CFTS CEs (5.0 Ωcm^2), and N–CCdTS-CEs (6.9 Ωcm^2) respectively. These results indicate that S-CFTS and S-CCdTS have the capability for faster electrocatalytic reduction of I_3^- to I^- ions in an electrolyte as compared to that N–CFTS CEs and N–CCdTS-CEs. However, it is less effective than Pt CE. The slightly higher R_s values of the CCTS and CFTS might be due to poor adhesion of the films to the FTO substrate. The results obtained from the EIS and CV analysis are in good agreement with the device performance.

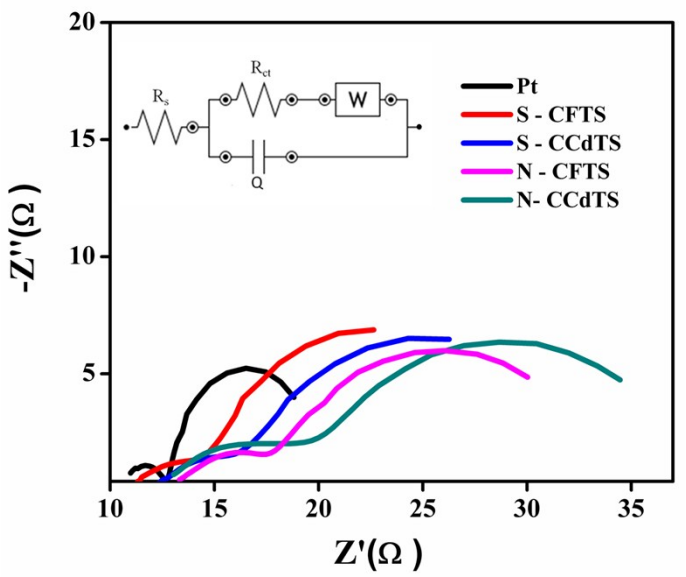

Fig.S6 EIS Spectra of symmetric cell fabricated with two identical CEs respectively

Tafel polarizations of symmetric cells were studied for further confirmation of the electrocatalytic activity of CEs for effective reduction of I_3^- to I^- ions in an electrolyte. The Tafel curves of symmetric cells of CEs are shown in Fig. S7. From the Tafel polarization analysis, exchange current density (J_0) can be obtained and correlated with the electrocatalytic activity of CEs. The curve in the lower potential region (|U|<120 mV) attributes to the polarization zone. The curve in the intermediate potential region corresponds to the Tafel zone. The curve at a higher potential corresponds to the diffusion zone.

In the Tafel zone, J_0 can be obtained from the intersection of the cathodic branch and the equilibrium potential line. The R_{ct} value of different CEs is calculated by using Eq. 1 [7].

$$\mathbf{J_o = RT/nFR_{ct}} \qquad \mathbf{2}$$

Where F is Faraday constant, T is temperature, n is the number of electrons exchanged in the reaction at the electrolyte-CE interface and R is gas constant.

The estimated J_o and R_{ct} values for different CEs from the Tafel polarization are summarized in Table S6. The R_{ct} value of different CEs calculated from EIS spectra and Tafel polarization curves are in good agreement (Table S6). The higher $J_{0,}$ smaller R_{ct} values of S–CFTS CEs and

S–CCdTS-CEs in contrast to N–CFTS CEs and N–CCdTS-CEs indicate that Sulfurized CEs have a better electrocatalytic activity to reduce I_3^- to I^- as compared with N- CEs.

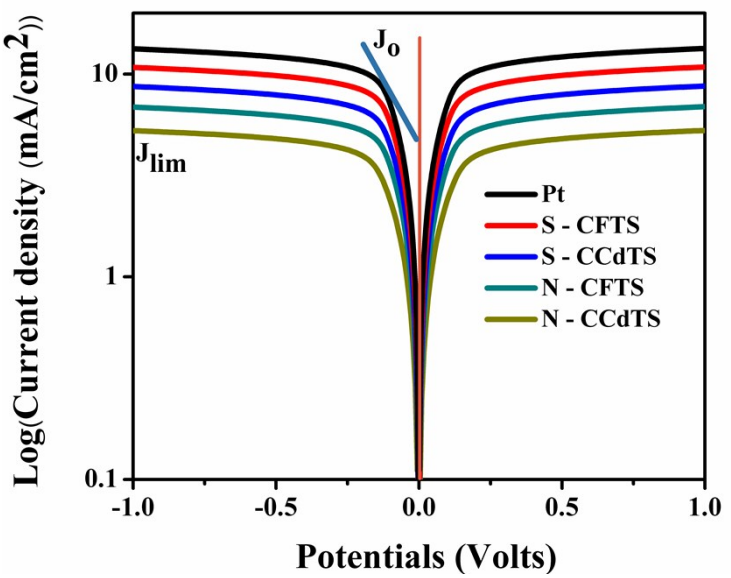

Fig. S7 Tafel plots of symmetric cell fabricated with two identical CEs respectively

Table S6 Electrochemical parameters obtained from EIS and Tafel polarization for different CEs

CE	Pt	S–CFTS	S–CCdTS	N–CFTS	N–CCdTS
R_s (Ω)[a]	10.9	11.37	12.30	13.2	12.4
R_{ct} (Ω)[a]	2.1	2.9	3.8	5.0	6.9
CPE(µF)[a]	42	38	39	34	32
R_{ct} (Ω)[b]	2.4	3.3	4.1	5.4	7.1
J_o(mA/cm^2) [b]	4.8	3.7	3.1	2.3	1.8

Photovoltaic parameters

Average (five cells) photovoltaic parameters of DSSCs with different counter electrodes

Table S7 Average solar cells parameters of DSSCs fabricated with Pt CEs.

CEs/	**J_{sc} ($_{mA/cm^2}$)**	**V_{oc} (mV)**	**FF**	**η (%)**
Pt/1st cell	18.00	712	0.60	8.10
Pt/2nd cell	17.78	712	0.59	7.98
Pt/3rd Cell	18.77	716	0.61	8.30
Pt/4th Cell	18.25	712	0.60	8.15
Pt/5th Cell	18.55	714	0.61	8.25
Average value	18.27	713.6	0.602	8.156
Standard deviation	0.312	1.28	0.0064	0.0952

Table S8 Average solar cells parameters of DSSCs fabricated with S–CFTS CEs.

CEs	**J_{sc} ($_{mA/cm^2}$)**	**V_{oc} (mV)**	**FF**	**η (%)**
S-CFTS/1st cell	17.10	706	0.56	7.25
S-CFTS/2nd cell	17.22	704	0.57	7.28
S-CFTS/3rd Cell	17.00	704	0.56	7.00
S-CFTS/4th Cell	17.90	706	0.57	7.40
S-CFTS/5th Cell	17.65	706	0.57	7.36
Average value	17.37	705.2	0.566	7.258
Standard deviation	0.32	0.96	0.0048	0.1064

Table S9 Average solar cells parameters of DSSCs fabricated with S–CCdTS CEs.

CEs	**J_{sc} ($_{mA/cm^2}$)**	**V_{oc} (mV)**	**FF**	**η (%)**
S-CCdTS/1st cell	16.85	698	0.57	7.24
S-CCdTS/2nd cell	16.35	696	0.56	7.15
S-CCdTS/3rd Cell	16.00	692	0.55	6.95
S-CCdTS/4th Cell	16.55	696	0.56	7.20
S-CCdTS/5th Cell	16.15	696	0.56	7.10
Average value	16.38	695.6	0.56	7.128
Standard deviation	0.256	1.44	0.004	0.082

Table S10 Average solar cells parameters of DSSCs fabricated with N–CFTS CEs.

CEs	**J_{sc} ($_{mA/cm^2}$)**	**V_{oc} (mV)**	**FF**	**η (%)**
N-CFTS/1st cell	14.30	683	0.54	5.72
N-CFTS/2nd cell	14.80	686	0.54	5.90
N-CFTS/3rd Cell	14.00	682	0.54	5.62
N-CFTS/4th Cell	14.55	686	0.54	5.70
N-CFTS/5th Cell	15.32	686	0.55	6.00
Average value	14.594	684.6	0.54	5.788
Standard deviation	0.3728	1.68	0.003	0.1296

Table S11 Average solar cells parameters of DSSCs fabricated with **N–CCdTS** CEs.

CEs	**J_{sc} ($_{mA/cm^2}$)**	**V_{oc} (mV)**	**FF**	**η (%)**
N-CCdTS/1st cell	12.90	672	0.53	5.10
N-CCdTS/2nd cell	13.35	676	0.53	5.38
N-CCdTS/3rd Cell	13.65	678	0.53	5.40
N-CCdTS/4th Cell	13.55	675	0.53	5.45
N-CCdTS/5th Cell	13.00	672	0.53	5.20
Average value	13.29	675	0.53	5.30
Standard deviation	0.272	2.08	0.004	0.0032